

AN ASYMPTOTIC ANALYSIS FOR A MODEL OF CHEMICAL VAPOR DEPOSITION ON A MICROSTRUCTURED SURFACE*

MATTHIAS K. GOBBERT[†] AND CHRISTIAN A. RINGHOFER[‡]

Abstract. We consider a model for chemical vapor deposition, the process of adsorption of gas onto a surface together with the associated deposition of a chemical reactant on the surface. The surface has a microscopic structure which, in the context of semiconductor manufacturing, arises from a preprocessing of the semiconductor wafer. Using singular perturbation analysis, a boundary condition for the corresponding diffusion equation is derived, which allows for the replacement of the microstructured surface by a flat boundary. The asymptotic analysis is numerically verified with a simple test example.

Key words. time-dependent initial-boundary value problem, homogenization, singular perturbation, mass transfer, chemically reacting flows, asymptotic analysis, microstructured surfaces, partial differential equations

AMS subject classifications. 65M06, 73B27, 76D30, 80A20, 80A32

PII. S0036139999528467X

1. Introduction. We consider the process of adsorption of the components of a chemically reacting flow onto a surface with a given microstructure. Our motivation for considering this problem is the coating of microstructured surfaces with thin films via chemical vapor deposition. In chemical vapor deposition a reacting gas flows through an inlet into a reactor. Inside, the reactor components of the gas are adsorbed onto the processed material, creating a thin surface layer. We are concerned with the case when the surface is patterned, i.e., exhibits a certain regular surface structure whose scale is much smaller than the scale of the reactor geometry. Chemical vapor deposition has a wide range of industrial applications. Our motivation arises from the use of chemical vapor deposition in processing semiconductor wafers. There, the surface structure arises from trenches, which are the result of prior processing of the wafer. These trenches, or features, are of the same order of magnitude as the future semiconductor devices (10^{-6}m to 10^{-7}m), while the whole wafer is usually 4 or 6 inches in diameter.

We will make the following assumptions on the flow and the geometry.

1. The reactor is assumed to work under high pressure conditions. This means that the mean free path of the flow is so small that the flow can be described by a diffusion process of the reacting gas through the background gas present in the reactor; see [LC]. In terms of that work, the Knudson number Kn , which is the ratio of the mean free path over the typical length scale, is assumed to be small, $\text{Kn} \ll 1$. Thus, the governing equations are of the form

$$(1.1) \quad \text{(a) } \partial_t \rho = -\text{div}_z F + R(\rho, z, t), \quad \text{(b) } F = -D(z, t) \nabla_z \rho,$$

*Received by the editors April 17, 1995; accepted for publication (in revised form) November 20, 1996; published electronically March 24, 1998. This research was supported by ARPA grant F49620-93-1-0062.

<http://www.siam.org/journals/siap/58-3/28467.html>

[†]Department of Mathematics, Arizona State University, Tempe, AZ 85287-1804. Current address: Department of Mathematics and Statistics, University of Maryland, Baltimore County, 1000 Hilltop Circle, Baltimore, MD 21250 (gobbert@math.umbc.edu).

[‡]Department of Mathematics, Arizona State University, Tempe, AZ 85287-1804 (ringhofer@asu.edu).

where z denotes the vector of spatial variables and t denotes time. The function ρ denotes the density of the reacting gas, and the vector F denotes the flux. The symmetric positive definite diffusion matrix D is assumed to be given. The matrix D can vary in space and time because of the presence of temperature gradients. Temperature is assumed to be a given quantity for the purpose of this paper. For practical applications, the presented analysis can be easily extended to include heat conduction, and a separate equation for the temperature can be augmented. The term $R(\rho, z, t)$ in (1.1(a)) models the reaction of the gas with the background in the flow phase.

2. The microstructured surface, which we will denote by Γ_a , is given by the equation

$$(1.2) \quad y = \tilde{h}_\varepsilon(x), \quad z = (x_1, x_2, y).$$

This assumption means that the growth of the surface is so slow compared to the time constant of the flow that it can be assumed to be independent of time. This is a realistic assumption, considering the surface grows at a time scale of minutes, while the particles of the flow move with the velocity of the flow. The mathematical treatment of an evolving fine structure is reserved for a future paper in preparation. The microstructure of the surface is modeled by the assumption that

$$(1.3) \quad \tilde{h}_\varepsilon(x) = \varepsilon h\left(x, \frac{x}{\varepsilon}\right)$$

holds, where ε is a small, dimensionless parameter. Notice that all quantities are already assumed to be dimensionless for the purposes of this analysis. Thus, a domain width of 1 unit in both x -variables can be assumed. The function $h(x, \xi)$ varies moderately in all its variables and is assumed to be periodic in the second variable ξ . So,

$$(1.4) \quad h(x, \xi + \mathbf{e}_1) = h(x, \xi + \mathbf{e}_2) = h(x, \xi)$$

holds for $\mathbf{e}_1 = (1, 0)^T$ and $\mathbf{e}_2 = (0, 1)^T$. The scale given by the parameter ε is usually referred to as the feature scale. Note that usually microstructured surfaces are assumed to be periodic if mechanical or optical properties are considered (see, for instance, [BR1], [BR2], [URE]). The assumption (1.4) means that “neighboring regions” of the surface look, in some sense, similar, while it allows us to prescribe, for instance, a different average trench depth in different areas of the adsorbing surface. The model as posed here is already dimensionless. In its original dimensional form, the parameter ε would correspond to the period of the features of, say, $1 \mu\text{m}$. If the overall size of the domain is, for instance, 1 cm, then the dimensionless ε could be chosen as their ratio of 10^{-4} .

More theoretical work concerning problems involving highly oscillating quantities include [CS], [DL], [KPV], [KV]. They and the references therein provide the theoretical framework for this work, which is meant as the first step towards a practical simulator for chemical vapor deposition in the context of semiconductor manufacturing. Therefore, this model for the wafer surface is the appropriate one for the application under consideration, and a more direct analysis is used than in those references.

3. The adsorption of gas onto the surface is given by the boundary condition

$$(1.5) \quad \nu \bullet F = S(\rho, z, t) \quad \text{for } z \in \Gamma_a,$$

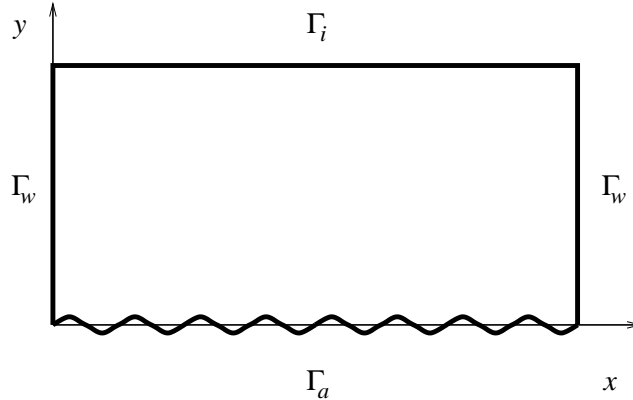


FIG. 1. Sketch of the two-dimensional domain with associated coordinate system.

where ν denotes the unit outward normal vector on the surface Γ_a . The function S in (1.5) models the deposition rate on the surface (see [LC], [CPGRJ]).

4. For the purpose of simplicity, we assume the geometry to be a cuboid, with the inlet taking up the top face and the adsorbing surface Γ_a occupying the bottom face. A sketch of the geometry is given in Figure 1.

On the top face Γ_t , the density ρ is prescribed, and on the side walls Γ_w , hard wall boundary conditions are imposed. So, altogether, the diffusion equation (1.1) is subject to the boundary conditions

$$(1.6(a)) \quad \rho(z, t) = \rho_b(z, t) \quad \text{for } z \in \Gamma_t,$$

$$(1.6(b)) \quad \nu \bullet F(z, t) = 0 \quad \text{for } z \in \Gamma_w,$$

$$(1.6(c)) \quad \nu \bullet F(z, t) = S(\rho, z, t) \quad \text{for } z \in \Gamma_a.$$

The problem addressed in this paper is a classical singular perturbation problem. The solution of the diffusion equation (1.1) poses no major challenge for modern computational tools. However, in order to accurately discretize the boundary condition (1.6(c)) at the adsorbing surface Γ_a , the surface structure would have to be resolved on a numerical mesh. Since the scale of the surface structure is five orders of magnitude smaller than that of the overall geometry, this is an impossible task, even for the most advanced adaptive grid refinement techniques. On the other hand, the structure of the surface can be expected to influence the flow only in a narrow region above Γ_a . We will use asymptotic analysis to derive a boundary condition which will allow us to replace the microstructured surface by a flat surface.

This paper is organized as follows.

In section 2 we will derive an approximate solution to the initial-boundary value problem (1.1)–(1.6), using asymptotics in the small, dimensionless parameter ε in (1.3). The outer solution, which is valid in the reactor away from the microstructured wafer surface Γ_a , will vary only on a slow spatial scale, since the effects of the microstructure will be smoothed out away from Γ_a due to the parabolicity of the differential equation (1.1). Close to the surface Γ_a , the solution will be corrected by a small layer term, which decays rapidly away from Γ_a . The matching conditions for

the inner and outer solutions result in an asymptotic boundary condition for the outer problem, given in (2.40), which only uses the average additional surface area produced by the microstructure. Thus, an approximate solution away from the surface Γ_a can be computed by using only a simple parameter function characterizing the surface, without resolving the wafer scale numerically.

In section 3 the asymptotic analysis of section 2 is verified numerically for a two-dimensional version of the above problem (i.e., for the case of a narrow channel). To this end, we choose a microstructure on the wafer surface whose scale is just large enough that it can be resolved using a nonuniform mesh. This scale is still three orders of magnitude larger than the one used in practical applications. This “true” solution is then compared to the solution of the asymptotic problem derived in section 2. The agreement of the densities and fluxes is as good as can be expected for the moderate numerical value of $\varepsilon = 1/16$ used.

2. Asymptotic expansion. In this section we will derive an asymptotic expansion of the solution of the initial boundary value problem (1.1)–(1.6) in powers of the small parameter ε in (1.3). ε describes to some extent the roughness of the adsorbing surface Γ_a . So, for $\varepsilon = 0$, Γ_a would become the flat surface given by $y = 0$, and the numerical solution of equation (1.1) would become straightforward. Since we expect the structure of the surface to influence the flow only in a narrow layer region directly above Γ_a , we make the following ansatz.

$$(2.1(a)) \quad \rho(z, t) = \tilde{\rho}_\varepsilon(z, t) + \bar{\rho}_\varepsilon \left(x, \frac{x}{\varepsilon}, \frac{y}{\varepsilon}, t \right), \quad z = (x_1, x_2, y),$$

$$(2.1(b)) \quad \tilde{\rho}_\varepsilon = \sum_{j=0}^{\infty} \tilde{\rho}_j(z, t) \varepsilon^j, \quad \bar{\rho}_\varepsilon = \sum_{j=0}^{\infty} \bar{\rho}_j \left(x, \frac{x}{\varepsilon}, \frac{y}{\varepsilon}, t \right) \varepsilon^j,$$

$$(2.1(c)) \quad F(z, t) = \tilde{F}_\varepsilon(z, t) + \bar{F}_\varepsilon \left(x, \frac{x}{\varepsilon}, \frac{y}{\varepsilon}, t \right),$$

$$(2.1(d)) \quad \tilde{F}_\varepsilon = \sum_{j=0}^{\infty} \tilde{F}_j(z, t) \varepsilon^j, \quad \bar{F}_\varepsilon = \sum_{j=-1}^{\infty} \bar{F}_j \left(x, \frac{x}{\varepsilon}, \frac{y}{\varepsilon}, t \right) \varepsilon^j.$$

An ansatz is made for both ρ and F in order to separate their effects on the asymptotics explicitly. The terms $\bar{\rho}$ and \bar{F} denote the layer corrections which only produce a significant contribution to the solution close to the adsorbing surface Γ_a . So,

$$(2.2) \quad (a) \quad \lim_{\eta \rightarrow \infty} \bar{\rho}_j(x, \xi, \eta, t) = 0, \quad (b) \quad \lim_{\eta \rightarrow \infty} \bar{F}_j(x, \xi, \eta, t) = 0 \quad \forall x, \xi, t, j$$

hold. Moreover, we assume the same periodicity properties for the layer correction terms $\bar{\rho}_\varepsilon$ and \bar{F}_ε as we do for the structure of the adsorbing surface Γ_a in (1.4). So,

$$(2.3(a)) \quad \bar{\rho}_j(x, \xi + \mathbf{e}_1, \eta, t) = \bar{\rho}_j(x, \xi + \mathbf{e}_2, \eta, t) = \bar{\rho}_j(x, \xi, \eta, t),$$

$$(2.3(b)) \quad \bar{F}_j(x, \xi + \mathbf{e}_1, \eta, t) = \bar{F}_j(x, \xi + \mathbf{e}_2, \eta, t) = \bar{F}_j(x, \xi, \eta, t)$$

hold, where $\mathbf{e}_1 = (1, 0)^T$ and $\mathbf{e}_2 = (0, 1)^T$ again. We first derive the equations for the zero-order term of the outer solution $\tilde{\rho}_0, \tilde{F}_0$. Fixing $y > 0$ and letting the parameter ε tend to zero yields

$$(2.4) \quad (a) \quad \partial_t \tilde{\rho}_0 = -\operatorname{div}_z \tilde{F}_0 + R(\tilde{\rho}_0, z, t), \quad (b) \quad \tilde{F}_0 = -D(z, t) \nabla_z \tilde{\rho}_0.$$

For the leading-order term of the layer correction $(\bar{\rho}_0, \bar{F}_{-1})$, we obtain by fixing $\eta = \frac{y}{\varepsilon}$ and letting ε go to zero

$$(2.5) \quad (a) \quad \operatorname{div}_{\xi, \eta} \bar{F}_{-1} = 0, \quad (b) \quad \bar{F}_{-1} = -D(x, y = 0, t) \nabla_{\xi, \eta} \bar{\rho}_0,$$

where

$$(2.6(a)) \quad \bar{F}_{-1} = (\bar{F}_{-1}^1, \bar{F}_{-1}^2, \bar{F}_{-1}^3)^T, \quad \operatorname{div}_{\xi, \eta} \bar{F}_{-1} = \partial_{\xi_1} \bar{F}_{-1}^1 + \partial_{\xi_2} \bar{F}_{-1}^2 + \partial_{\eta} \bar{F}_{-1}^3,$$

$$(2.6(b)) \quad \nabla_{\xi, \eta} \bar{\rho}_0 = (\partial_{\xi_1} \bar{\rho}_0, \partial_{\xi_2} \bar{\rho}_0, \partial_{\eta} \bar{\rho}_0)^T$$

hold. Note that the expansion for \bar{F}_{ε} in (2.1(d)) has to start with the $O(\frac{1}{\varepsilon})$ term in order to close the system.

Turning to the boundary condition (1.6(c)), we first compute the normal vector ν using (1.3). Thus, ν is given by

$$(2.7(a)) \quad \nu = \frac{1}{\sigma} [\varepsilon \tilde{\nu} + \bar{\nu}], \quad \tilde{\nu} = \begin{pmatrix} \partial_{x_1} h \\ \partial_{x_2} h \\ 0 \end{pmatrix}, \quad \bar{\nu} = \begin{pmatrix} \partial_{\xi_1} h \\ \partial_{\xi_2} h \\ -1 \end{pmatrix},$$

$$(2.7(b)) \quad \sigma^2 = 1 + (\varepsilon \partial_{x_1} h + \partial_{\xi_1} h)^2 + (\varepsilon \partial_{x_2} h + \partial_{\xi_2} h)^2,$$

and the boundary condition (1.6(c)) becomes in leading ($= O(\frac{1}{\varepsilon})$) order

$$(2.8) \quad \bar{\nu} \bullet \bar{F}_{-1} = 0.$$

Combining (2.5(a)) and (2.5(b)), we see that the zero-order layer correction term $\bar{\rho}_0$ satisfies the homogeneous diffusion equation

$$(2.9) \quad \operatorname{div}_{\xi, \eta} [D(x, y = 0, t) \nabla_{\xi, \eta} \bar{\rho}_0] = 0$$

together with the boundary conditions

$$(2.10) \quad \bar{\nu}^T D \nabla_{\xi, \eta} \bar{\rho}_0 = 0 \quad \text{for } \eta = h(x, \xi),$$

the homogeneous boundary conditions at the hard walls Γ_w , and the decay condition (2.2(a)) at $\eta = \infty$. An easy application of the maximum principle or, alternatively, a standard L^2 -estimate immediately shows that the term $\bar{\rho}_0$ vanishes identically. Thus,

$$(2.11) \quad \bar{\rho}_0(x, \xi, \eta, t) = 0, \quad \bar{F}_{-1}(x, \xi, \eta, t) = 0 \quad \forall x, \xi, \eta, t$$

hold. Therefore, no significant correction to the density is present close to the adsorbing surface Γ_a , and the flow will stay bounded as $\varepsilon \rightarrow 0$. However, as we will see, there is a significant correction to the flux F close to the adsorbing surface, caused by the microstructure of Γ_a . Going to the next higher-order term in the layer expansion yields

$$(2.12) \quad (a) \quad \operatorname{div}_{\xi, \eta} \bar{F}_0 = 0, \quad (b) \quad \bar{F}_0 = -D(x, y = 0, t) \nabla_{\xi, \eta} \bar{\rho}_1$$

together with the boundary conditions

$$(2.13) \quad \bar{\nu} \bullet [\bar{F}_0 + \tilde{F}_0] = S(\bar{\rho}_0, x, y = 0, t) \sigma_0,$$

where the terms \tilde{F}_0 and $\tilde{\rho}_0$ are evaluated at $y = 0$ and the layer correction term \bar{F}_0 is evaluated at $\eta = h(x, \xi)$. The coefficient σ_0 in (2.13) is given by

$$(2.14) \quad \sigma_0^2 = 1 + (\partial_{\xi_1} h)^2 + (\partial_{\xi_2} h)^2.$$

Thus, after computing the zero-order term of the outer solution $(\tilde{\rho}_0, \tilde{F}_0)$, the layer correction term $(\bar{\rho}_1, \bar{F}_0)$ is given as the solution of the homogeneous quasi steady state diffusion equation (2.12) together with the boundary condition (2.13) at Γ_a , appropriate homogeneous boundary conditions at the hard walls Γ_w , and the decay condition (2.2).

The goal of the asymptotic analysis is, of course, to decouple the boundary value problem for the outer solution $(\tilde{\rho}_0, \tilde{F}_0)$ from the layer expansion. To this end we first characterize all the solutions of the layer equation (2.12), which satisfy the decay condition (2.2). We have the following lemma.

LEMMA 2.1. *Let the symmetric positive definite matrix function $D(x, t) \in R^{3 \times 3}$ be given by*

$$(2.15) \quad D = \begin{pmatrix} D_0 & d \\ d^T & \delta \end{pmatrix},$$

where $D_0 \in R^{2 \times 2}$, $d \in R^2$, and $\delta \in R$ hold. Then, all solutions $\rho(x, \xi, \eta, t)$ of the diffusion equation

$$(2.16) \quad \operatorname{div}_{\xi, \eta}[D(x, t)\nabla_{\xi, \eta}\rho] = 0,$$

which are periodic with period 1 in the variable ξ and satisfy $\lim_{\eta \rightarrow \infty} \rho = 0$, are of the form

$$(2.17) \quad \rho(x, \xi, \eta, t) = \sum_{n \in Z^2} g_n(x, t) \exp[2\pi i n^T \xi - 2\pi K_n(x, t)\eta]$$

with

$$(2.18) \quad K_n(x, t) = \frac{1}{\delta} \left[i n^T d + \sqrt{\delta n^T D_0 n - (n^T d)^2} \right], \quad n = (n_1, n_2)^T,$$

where the term under the square root in (2.18) is always positive.

Proof. Since the function ρ is periodic in ξ , a Fourier expansion in the variable ξ ,

$$(2.19) \quad \rho(x, \xi, \eta, t) = \sum_{n \in Z^2} \tilde{g}_n(x, \eta, t) \exp[2\pi i n^T \xi],$$

has to hold. Inserting (2.19) into the differential equation (2.16) yields

$$(2.20) \quad D\nabla_{\xi, \eta}\rho = \sum_{n \in Z^2} \begin{pmatrix} 2i\pi\tilde{g}_n D_0 n + \partial_\eta \tilde{g}_n d \\ 2i\pi\tilde{g}_n d^T n + \partial_\eta \tilde{g}_n \delta \end{pmatrix} \exp[2\pi i n^T \xi],$$

$$\operatorname{div}_{\xi, \eta} D\nabla_{\xi, \eta}\rho = \sum_{n \in Z^2} \{2i\pi n^T [2i\pi\tilde{g}_n D_0 n + \partial_\eta \tilde{g}_n d] + \partial_\eta [2i\pi\tilde{g}_n d^T n + \partial_\eta \tilde{g}_n \delta]\} \exp[2\pi i n^T \xi],$$

$$(2.21)$$

and therefore

$$(2.22) \quad \delta \partial_\eta^2 \tilde{g}_n + 4i\pi n^T d \partial_\eta \tilde{g}_n - 4\pi^2 n^T D_0 n \tilde{g}_n = 0.$$

Since the coefficients of this differential equation are independent of η , the solutions are of the form

$$(2.23) \quad \tilde{g}_n = g_n \exp(-2\pi K_n \eta),$$

where K_n depends on all variables except η (and ξ). Inserting (2.25) into (2.24) gives the quadratic equation

$$(2.24) \quad \delta K_n^2 - 2in^T d K_n - n^T D_0 n = 0$$

with solutions

$$(2.25) \quad K = \frac{1}{\delta} \left[in^T d \pm \sqrt{\delta n^T D_0 n - (n^T d)^2} \right].$$

The term under the square root is always positive, since it can be written as

$$(2.26) \quad \frac{1}{\delta} (\delta n^T, -n^T d) \begin{pmatrix} D_0 & d \\ d^T & \delta \end{pmatrix} \begin{pmatrix} \delta n \\ -n^T d \end{pmatrix}.$$

Hence, the square root is real and the positive sign has to be taken in (2.27) to obtain a solution, which decays to zero as $\eta \rightarrow \infty$. \square

With the help of the characterization of exponentially decaying solutions of the diffusion equation given in Lemma 2.1, we can now derive a solvability condition for the boundary condition (2.13). Collecting the layer correction terms in (2.13) on the left-hand side yields

$$(2.27) \quad -\bar{\nu} \bullet D \nabla_{\xi, \eta} \bar{\rho}_1(x, \xi, \eta = h(x, \xi), t) = \sigma_0 S - \bar{\nu} \bullet \tilde{F}_0, \quad \bar{\nu} = \begin{pmatrix} \partial_{\xi_1} h \\ \partial_{\xi_2} h \\ -1 \end{pmatrix}.$$

The next lemma gives a necessary condition for the solution of equation (2.27), where the function $f(x, \xi, t)$ will later be replaced by the right-hand side in (2.27).

LEMMA 2.2. *Let the symmetric, positive definite matrix D be partitioned as in (2.15). Then the equation*

$$(2.28) \quad \bar{\nu}^T D \nabla_{\xi, \eta} \rho(x, \xi, \eta = h(x, \xi), t) = f(x, \xi, t),$$

where the function $f(x, \xi, t)$ is periodic with period 1 in the variable ξ , has a solution of the form

$$(2.29) \quad \rho(x, \xi, \eta = h(x, \xi), t) = \sum_{n \in Z^2} g_n(x, t) \exp[2\pi in^T \xi - 2\pi K_n(x, t)h(x, \xi)]$$

only if

$$(2.30) \quad \int_0^1 d\xi_1 \int_0^1 d\xi_2 f(x, \xi, t) = 0$$

holds for all values of x and t .

Proof. Inserting the expression (2.29) into (2.28) yields

$$(2.31) \quad \bar{\nu}^T D \nabla_{\xi, \eta} \rho|_{\eta=h(x, \xi)} = 2\pi \sum_{n \in Z^2} g_n (\nabla_{\xi} h^T, -1) D \begin{pmatrix} in \\ -K_n \end{pmatrix} \exp[2\pi in^T \xi - 2\pi K_n h(x, \xi)].$$

Next, we try to write the coefficients in the sum (2.31) as

$$(2.32) \quad (\nabla_\xi h^T, -1)D \begin{pmatrix} in \\ -K_n \end{pmatrix} = u_n^T(in - K_n \nabla_\xi h),$$

with some vectors $u_n \in R^2$ independent of the variable ξ . Assuming the partition (2.15) of the matrix D , (2.32) gives

$$(2.33) \quad \nabla_\xi h^T(iD_0 n - K_n d) - id^T n + \delta K_n = u_n^T(in - K_n \nabla_\xi h).$$

Separating the terms which are dependent on ξ from the others in equation (2.33) yields the equations

$$(2.34) \quad (a) \quad iD_0 n - K_n d = -K_n u_n, \quad (b) \quad -id^T n + \delta K_n = in^T u_n.$$

Computing the vector u_n from (2.34(a)) and inserting into (2.34(b)) yields

$$(2.35) \quad -id^T n + \delta K_n = \frac{i}{K_n} n^T (K_n d - iD_0 n),$$

which is the same as equation (2.24) used to determine K_n . Hence, we can use the vectors u_n given by (2.34(a)) to rewrite (2.31) as

$$(2.36) \quad \begin{aligned} \tilde{v}^T D \nabla_{\xi, \eta} |_{\eta=h(x, \xi)} &= 2\pi \sum_{n \in Z^2} g_n u_n^T (in - K_n \nabla_\xi h) \exp[2\pi in^T \xi - 2\pi K_n h(x, \xi)] \\ &= \operatorname{div}_\xi \left\{ \sum_{n \in Z^2} g_n u_n \exp[2\pi in^T \xi - 2\pi K_n h(x, \xi)] \right\}. \end{aligned}$$

Hence, we can write the left-hand side of (2.28) as the divergence of a vector-valued function which is 1-periodic in the variable ξ . Therefore, the integral (2.30) has to vanish identically for (2.28) to have a solution. \square

It should be pointed out that (2.30) is only a necessary condition for the existence of the solution to (2.28). Thus, we can conclude that, if the solution of the full problem (1.1)–(1.6) possesses an expansion of the form (2.1), then the zero-order terms $(\tilde{\rho}_0, \tilde{F}_0)$ have to be compatible with (2.30).

In order to show the existence of solutions to the layer problem (2.28), it would be necessary to show the completeness of the basis functions of the form $\phi_n(\xi) = \exp[2\pi in^T \xi - 2\pi K_n h(x, \xi)]$ in the space of 1-periodic L^2 -functions of ξ . Even then, the existence of layer solutions is a quite delicate problem, since the coefficients of the form $(\nabla_\xi h^T, -1)D(in, -K_n)^T$ would have to be nonzero for sufficiently large $\|n\|$ in order to avoid resonance. Existence and the asymptotic validity of the expansion for the layer solution will be the topic of a subsequent paper.

Using the necessary solvability condition from Lemma 2.2, we can now separate the boundary value problem defining the outer solution $(\tilde{\rho}_0, \tilde{F}_0)$ from the one defining the boundary layer correction term $(\tilde{\rho}_1, \tilde{F}_1)$. We have the following theorem.

THEOREM 2.3. *The zero-order term $(\tilde{\rho}_0, \tilde{F}_0)$ of the expansion of the outer solution satisfies the boundary condition*

$$(2.37) \quad \mathbf{e}_3 \bullet \tilde{F}_0 = \tilde{\sigma} S(\tilde{\rho}_0, x, y = 0, t),$$

where $(\tilde{\rho}_0, \tilde{F}_0)$ are evaluated at $y = 0$, \mathbf{e}_3 denotes the third unit vector $(0, 0, 1)^T$, and $\tilde{\sigma}$ is given by

$$(2.38) \quad \tilde{\sigma}(x) = \int_0^1 d\xi_1 \int_0^1 d\xi_2 \sigma_0(x, \xi), \quad \sigma_0^2 = 1 + (\partial_{\xi_1} h)^2 + (\partial_{\xi_2} h)^2.$$

Proof. Rewriting the boundary condition (2.13) gives

$$(2.39) \quad -\tilde{\nu}^T D \nabla_{\xi, \eta} \tilde{\rho}_1 = \sigma_0 S - \tilde{\nu} \bullet \tilde{F}_0.$$

The necessary condition of Lemma 2.2 implies that the integral over ξ of the right-hand side must vanish. Evaluating the integrals and defining $\tilde{\sigma}$ as in (2.38) yields (2.37). \square

So, in summary, the zero-order expansion term of the outer solution $(\tilde{\rho}_0, \tilde{F}_0)$ is given as the solution of the problem

$$(2.40(a)) \quad \partial_t \tilde{\rho}_0 = -\text{div}_z \tilde{F}_0 + R(\tilde{\rho}_0, z, t), \quad \tilde{F}_0 = -D(z, t) \nabla_z \tilde{\rho}_0$$

together with the boundary conditions

$$(2.40(b)) \quad \tilde{\rho}_0(z, t) = \rho_b(z, t) \quad \text{for } z \in \Gamma_t,$$

$$(2.40(c)) \quad \nu \bullet \tilde{F}_0(z, t) = 0 \quad \text{for } z \in \Gamma_w,$$

$$(2.40(d)) \quad \mathbf{e}_3 \bullet \tilde{F}_0 = \tilde{\sigma} S(\tilde{\rho}_0, z, t) \quad \text{for } z \in \Gamma_a,$$

where $\tilde{\sigma}$ is defined as in (2.38). The term $\tilde{\sigma}$ reflects the increased surface area due to the roughness of the adsorbing surface Γ_a .

The boundary layer correction close to Γ_a is given by the correction term $(\bar{\rho}_1, \bar{F}_0)$, which is the solution of the problem

$$(2.41(a)) \quad \text{div}_{\xi, \eta} \bar{F}_0 = 0, \quad \bar{F}_0 = -D(x, y = 0, t) \nabla_{\xi, \eta} \bar{\rho}_1$$

together with the boundary condition

$$(2.41(b)) \quad \tilde{\nu} \bullet [\bar{F}_0 + \tilde{F}_0] = S(\bar{\rho}_0, x, y = 0, t) \sigma_0,$$

the conditions

$$(2.41(c)) \quad \lim_{\eta \rightarrow \infty} \bar{\rho}_1(x, \xi, \eta, t) = 0, \quad \lim_{\eta \rightarrow \infty} \bar{F}_0(x, \xi, \eta, t) = 0 \quad \forall x, \xi, t, j,$$

and the condition of periodicity in the variable ξ . Higher-order terms in the expansion can be derived in the same manner and could be used as a higher-order correction to the solution.

3. Numerical results. This section will demonstrate that the problem formulation given by (2.40) is correct by comparing the solution with one obtained by using a finite difference method on the original problem (1.1). Since the ultimate purpose of this problem is to serve as an interface between the associated reactor scale and feature scale models, the quality of the solutions obtained will be compared in two ways. First, the method has to be able to predict the density ρ correctly in the bulk of the

domain in order to facilitate the interaction with the reactor scale model. Second, the model has to predict the flux of gases into the wafer surface correctly. However, this does not have to hold on the scale of the microstructure, since this will be modeled by the feature scale model itself, but rather, the average flux into the wafer has to be predicted correctly.

For the physical problem at hand it is customary to assume an infinite trench length in the x_2 -direction. Hence, the remaining problem is two-dimensional in the independent variables $x := x_1$ and y , and hence z stands now for the vector $(x, y)^T$. The test problem used is then

$$(3.1) \quad (a) \quad \partial_t \rho = -\operatorname{div}_z(F) + R(\rho, z, t), \quad (b) \quad F = -D(z, t) \nabla_z \rho$$

on the domain

$$(3.2) \quad \Omega_z = \left\{ (x, y) \in \mathbb{R}^2 : 0 < x < 1, \tilde{h}_\varepsilon(x) < y < 1 \right\}$$

and with the boundary conditions

$$(3.3(a)) \quad \nu \bullet (-D \nabla_z \rho) = 0, \quad \nu = (-1, 0)^T \quad \text{for } x = 0,$$

$$(3.3(b)) \quad \nu \bullet (-D \nabla_z \rho) = 0, \quad \nu = (1, 0)^T \quad \text{for } x = 1,$$

$$(3.3(c)) \quad \rho = \rho_b(x, t) \quad \text{for } y = 1,$$

$$(3.3(d)) \quad \nu \bullet (-D \nabla_z \rho) = S(\rho, x, t), \quad \nu = (1/\sigma)(\partial_x \tilde{h}_\varepsilon, -1)^T \quad \text{for } y = \tilde{h}_\varepsilon(x)$$

for the initial condition

$$(3.4) \quad \rho(x, y, t = 0) = \rho_0(x, y).$$

The boundary conditions are realistic for modeling hard walls on the sides of the domain, a Dirichlet condition towards the interior of the reactor, and a flux condition on the wafer surface.

For convenience, the problem obtained by asymptotic analysis of the above problem is restated here in its two-dimensional form as

$$(3.5) \quad (a) \quad \partial_t \rho = -\operatorname{div}_{xy}(F) + R(\rho, x, y, t), \quad (b) \quad F = -D(x, y, t) \nabla_{xy} \rho$$

on the domain

$$(3.6) \quad \Omega_{xy} = \left\{ (x, y) \in \mathbb{R}^2 : 0 < x < 1, 0 < y < 1 \right\}$$

with boundary conditions

$$(3.7) \quad (a) \quad (-D \nabla_{xy} \rho)^1 = 0 \quad \text{for } x = 0, \quad (b) \quad (-D \nabla_{xy} \rho)^1 = 0 \quad \text{for } x = 1,$$

$$(c) \quad \rho = \rho_b(x, t) \quad \text{for } y = 1, \quad (d) \quad (-D \nabla_{xy} \rho)^2 = -\tilde{\sigma} S(\rho, x, t) \quad \text{for } y = 0$$

with

$$(3.8) \quad \tilde{\sigma}(x) = \int_0^1 \sigma_0(x, \xi) d\xi, \quad \sigma_0^2 = 1 + (\partial_\xi h)^2$$

and the initial condition

$$(3.9) \quad \rho(x, y, t = 0) = \rho_0(x, y).$$

This problem is solved by a finite difference method applied on a staggered grid on the unit square Ω_{xy} using a conservative formulation of the differential equation to ensure mass conservation of the chemical material.

To this end the grid points in the x -direction are defined as $x_i = i \Delta x$, $i = 0, \dots, I$, with $\Delta x = 1/I$ for some even integer $I \geq 2$. Similarly, in the y -direction, they are defined as $y_j = j \Delta y$, $j = 0, \dots, J$, with $\Delta y = 1/J$ for some even integer $J \geq 2$. On this grid we then define the approximations $v_{ij} \approx \rho(x_i, y_j, t)$ and $v_{ij}^{old} \approx \rho(x_i, y_j, t - \Delta t)$. We will also use as short-hand notation $F_{ij} := F(x_i, y_j, t)$, etc. Moreover, to avoid confusion with subscripts indicating a location on the grid, component indices are written as superscripts, so, for instance, $D_{i,j}^{11}$ is the (1,1)-element of the matrix $D(x_i, y_j, t)$. Also, for every grid point we define a differential domain

$$(3.10) \quad \Omega_{ij} := (x_{i-1}, x_{i+1}) \times (y_{j-1}, y_{j+1}) = \{(x, y) \in \mathbb{R}^2 : x_{i-1} < x < x_{i+1}, y_{j-1} < y < y_{j+1}\}.$$

Notice for later use that its size is $\mu(\Omega_{ij}) = (2 \Delta x)(2 \Delta y) = 4 \Delta x \Delta y$.

To get the conservative formulation, the differential equation is integrated over the differential domain Ω_{ij} centered at (x_i, y_j) . All integrals not involving spatial derivatives are then approximated by their integrands evaluated at (x_i, y_j) times the size of Ω_{ij} , namely, $\mu(\Omega_{ij}) = 4 \Delta x \Delta y$. The integral of the divergence term is converted into a surface integral by the Gauss integral theorem. Thus, we have after dividing by $4 \Delta x \Delta y$:

$$(3.11) \quad \frac{v_{ij} - v_{ij}^{old}}{\Delta t} = \frac{1}{4 \Delta x \Delta y} \int_{\partial \Omega_{ij}} \nu \bullet F \, d\sigma + R_{ij}.$$

Here, the implicit Euler method has been applied to avoid stability restrictions. The remaining integral is now approximated by

$$(3.12) \quad \int_{\partial \Omega_{ij}} \nu \bullet F \, d\sigma = 2 \Delta y (F_{i+1,j}^1 - F_{i-1,j}^1) + 2 \Delta x (F_{i,j+1}^2 - F_{i,j-1}^2).$$

This discretization is called conservative, since the mass initially present in the system is conserved. That is achieved because, using this discretization, the sum of all fluxes in the domain is equal to the flux through the boundary of the domain, that is,

$$(3.13) \quad \sum_{(i,j)} \int_{\partial \Omega_{ij}} \nu \bullet F \, d\sigma = \int_{\partial \Omega_{xy}} \nu \bullet F \, d\sigma.$$

Notice that the fluxes are never explicitly computed in the code. Instead, $F_{i+1,j}^1$, for instance, is further discretized using centered differences to get

$$(3.14) \quad F_{i+1,j}^1 = (-D \nabla_{xy} \rho)_{i,j}^1 = -D_{i+1,j}^{11} \left(\frac{\partial \rho}{\partial x} \right)_{i+1,j} - D_{i+1,j}^{12} \left(\frac{\partial \rho}{\partial y} \right)_{i+1,j}$$

$$(3.15) \quad \approx -D_{i+1,j}^{11} \frac{v_{i+2,j} - v_{i,j}}{2 \Delta x} - D_{i+1,j}^{12} \frac{v_{i,j+1} - v_{i,j-1}}{2 \Delta y}.$$

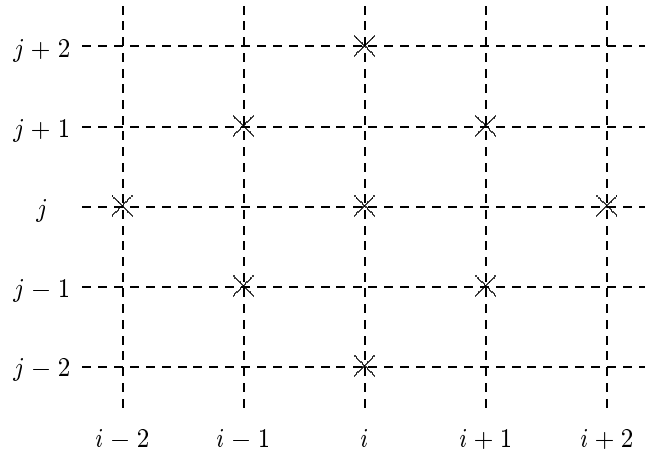


FIG. 2. *Nine-point stencil at (i, j) rotated by 45° .*

Observe that the resulting overall discretization has a nine-point stencil rotated by 45° , as shown in Figure 2. Therefore, the actual numerical domain is the staggered grid generated by

$$(3.16) \quad \tilde{\Omega} := \{(x_i, y_j) \in \Omega_{xy} : i + j \text{ even}\}.$$

This discretization results in a banded linear system of equations, which is solved by routines from LINPACK. Finally, the integral needed in the computation of $\tilde{\sigma}$ is approximated by the trapezoidal rule with interval width $\Delta\xi := \Delta x = 1/I$.

To validate the solution of the asymptotic problem, the classical problem is solved directly using a grid fine enough to discretize every period of $h(x, \xi)$ by at least eight points. Practically, this is implemented by introducing the transformation

$$(3.17) \quad \begin{pmatrix} x \\ y \end{pmatrix} = \begin{pmatrix} x \\ g(x, w) \end{pmatrix}$$

such that

$$(3.18) \quad (x, w) \in \Omega_{xw} = \{(x, w) \in \mathbb{R}^2 : 0 < x < 1, 0 < w < 1\}.$$

This transformation will achieve two goals. On the one hand, it transforms the domain of the problem to the unit square so that the boundary can be discretized easily. On the other hand, it also distributes the grid points in the y -direction in a nonuniform way such that more grid points lie closer to the surface than in the bulk. See Figure 3 for an example of a grid point distribution in the original domain Ω_z .

The solution procedure applied to the transformed domain Ω_{xw} is exactly the same as the one applied to the asymptotic problem Ω_{xy} .

The results presented below are for the following mathematical test problem:

$$(3.19) \quad D(x, y, t) = \begin{pmatrix} 2 & -1 \\ -1 & 2 \end{pmatrix}, \quad R(\rho, x, y, t) = -24x + 13,$$

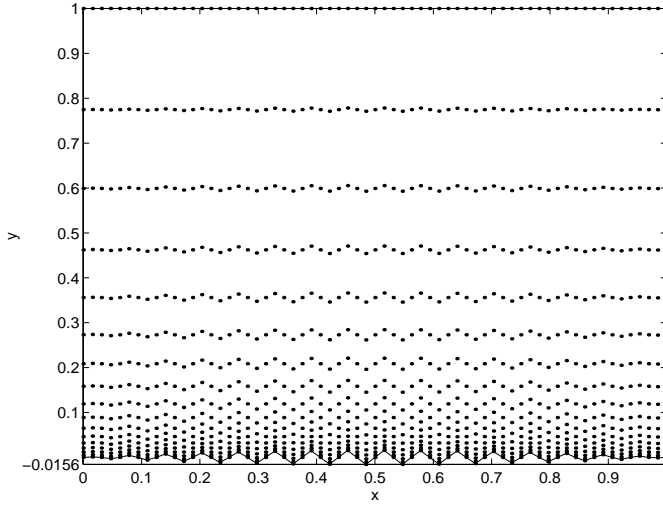


FIG. 3. Graph of the numerical domain with fewer grid points for clarity.

$$(3.20) \quad (a) \quad \rho_b(x, t) = 2x^3 - 3x^2 + t + 2,$$

$$(b) \quad S(\rho, x, t) = -6x^2 + 6x + 2, \quad (c) \quad \rho_0(x, y) = 2x^3 - 3x^2 + y + 1.$$

The surface model is chosen to give fast oscillations around a slowly varying carrier function, namely, as

$$(3.21) \quad y = \tilde{h}_\varepsilon(x) = \varepsilon h(x, x/\varepsilon) \quad \text{with} \quad h(x, \xi) = x(1 - x) \sin(\omega_0 \xi).$$

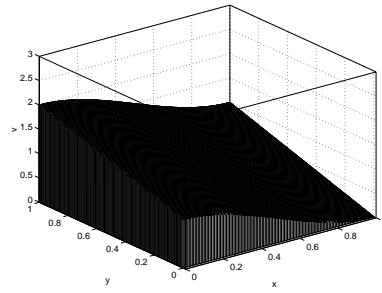
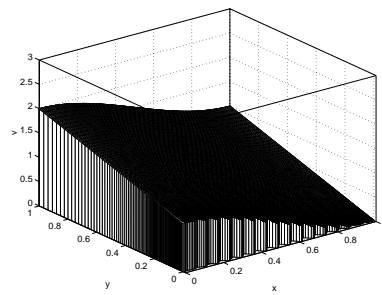
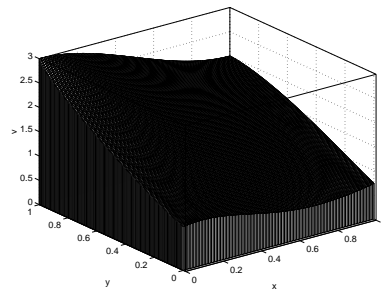
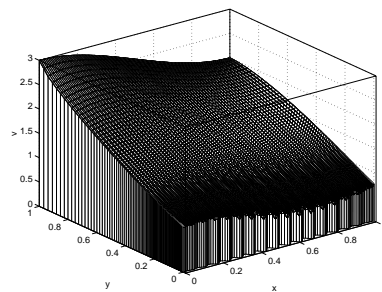
The values chosen for ε in the test problem is $\varepsilon = 1/16 = 0.0625$.

Finally, the transformation from (x, y) to (x, w) in the validation problem is chosen as

$$(3.22) \quad y = g(x, w) = \tilde{h}_\varepsilon(x) \frac{e^\alpha - e^{\alpha w}}{e^\alpha - 1} + \frac{e^{\alpha w} - 1}{e^\alpha - 1}.$$

The parameter in the transformation is chosen as $\alpha = 4$. The grid is chosen by $I = J = 128$ and the time step is $\Delta t = 0.01$. 100 steps are then computed to reach the final time $t_{final} = 1$.

The initial condition for the asymptotic problem is shown in Figure 4, and for the validation problem, in Figure 5. The solutions at the final time are presented in surface plots in Figures 6 and 7, respectively. To facilitate a comparison between both solutions Figure 8 shows a contour plot of both final solutions. The solid line represents the solution obtained from the asymptotic problem, while the dotted lines belong to the solution from the validation problem. Not surprisingly, the solution of the validation problem introduced some oscillations, which die out towards the upper boundary of the domain. Clearly, both solutions agree perfectly in the bulk of the domain except for these small oscillations.

FIG. 4. *Initial condition for the asymptotic problem.*FIG. 5. *Initial condition for the validation problem.*FIG. 6. *Final solution of the asymptotic problem.*FIG. 7. *Final solution of the validation problem.*

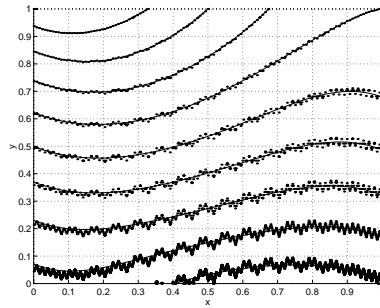


FIG. 8. Contour plot of both final solutions.

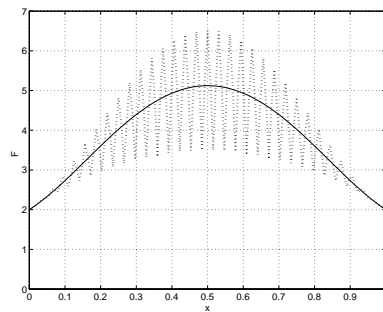


FIG. 9. Comparison of the final fluxes into the surface.

The second criterion for the quality of the approximation is its capability to predict the fluxes into the wafer surface. To this end the total flux into the surface,

$$(3.23) \quad F_{total} = \int_0^1 \nu \bullet F dx,$$

has been computed to $F_{total} = 3.85529763$ for the asymptotic model and to $F_{total} = 3.85490895$ for the validation problem. This is clearly in agreement. Moreover, Figure 9 shows the predicted fluxes vs. x along the surface. The solid line is computed from the asymptotic model, and the dotted line, from the validation model. Again, we observe the oscillations associated with the resolution of the actual surface structure. Clearly though, the average local fluxes are predicted correctly by the asymptotic model. This is as desired, since an associated feature scale model would only use these averages.

REFERENCES

- [BR1] O. BRUNO AND F. REITICH, *Numerical solution of diffraction problems: A method of variation of boundaries*, J. Opt. Soc. Amer. A, 10 (1993), pp. 1168–1175.
- [BR2] O. BRUNO AND F. REITICH, *Solution of a boundary value problem for Helmholtz equations via variation of the boundary into the complex domain*, in Proc. Roy. Soc. Edinburgh, 122A (1992), pp. 317–340.
- [CPGRJ] T. CALE, J. PARK, T. GANDY, G. RAUPP, AND M. JAIN, *Step coverage predictions using combined feature and reactor scale models for blanket tungsten LPCVD*, Chem. Eng. Comm., 119 (1993), pp. 197–220.

- [CS] D. CIORANESCU AND J. SAINT JEAN PAULIN, *Homogenization in open sets with holes*, J. Math. Anal. Appl., 71 (1979), pp. 590–607.
- [DL] A. DAMLAMIAN AND LI TA-TSIEN, *Boundary homogenization for elliptic problems*, J. Math. Pure Appl., 66 (1987), pp. 351–362.
- [KPV] W. KOHLER, G. PAPANICOLAOU, AND S. VARADHAN, *Boundary and interface problems in regions with very rough boundaries*, in Multiple Scattering and Waves in Random Media, P. L. Chow, W. E. Kohler, and G. C. Papanicolaou, eds., North-Holland, Amsterdam, 1981, pp. 165–197.
- [KV] R. KOHN AND M. VOGELIUS, *A new model for thin plates with rapidly varying thickness*, Internat. J. Solids Structures, 20 (1984), pp. 333–350.
- [LC] H. LIAO AND T. CALE, *Low Knudsen number transport and deposition*, J. Vac. Sci. Tech., A12 (1994), pp. 1020–1026.
- [URE] J. URETSKY, *The scattering of plain waves from periodic surfaces*, Ann. Phys., 33 (1965), pp. 400–427.